Macromolecules
ARTICLE

Macromolecules **2009**, *42*, 6953–6963 **6953**
DOI: 10.1021/ma901210u

Kinetic and Mechanistic Aspects of Ethylene and Acrylates Catalytic Copolymerization in Solution and in Emulsion

Kirill M. Skupov,[†] Jason Hobbs,[†] Pooja Marella,[†] David Conner,[‡] Suzanne Golisz,[‡] Brian L. Goodall,[‡] and Jerome P. Claverie*,[†]

[†]*NanoQAM Research Center, Quebec Center for Functional Materials, Department of Chemistry, University of Quebec at Montreal, 2101 rue Jeanne-Mance, CP8888, Montreal, Quebec H3C 3P8, Canada, and* [‡]*Emerging Technology Department, Rohm and Haas Company, 727 Norristown Road, Spring House, Pennsylvania 19477*

Received June 5, 2009; Revised Manuscript Received August 13, 2009

ABSTRACT: Ethylene was copolymerized with acrylates in solution and in emulsion using sulfonated arylphosphine Pd-based catalysts. The copolymerization of C_2H_4 and methyl acrylate in toluene was slowed by the σ-coordination of the acrylate on Pd. The substitution of pyridine by itself was shown to proceed via an associative mechanism with activation parameters $\Delta H^{\ddagger} = 16.8$ kJ/mol and $\Delta S^{\ddagger} = -98$ J mol^{-1} K^{-1} whereas the activation parameters for the substitution of pyridine by methyl acrylate were found to be $\Delta H^{\ddagger} = 18.1$ kJ/mol and $\Delta S^{\ddagger} = -87$ J mol^{-1} K^{-1}. Using these Pd-based catalysts in an emulsion polymerization process, latexes of copolymers of ethylene with various acrylates having particle diameters ~200 nm were obtained for the first time. Their solid contents did not exceed 5% because of the low activity of the catalyst resulting from the coordination of water and from the slow decomposition of the active site by water.

1. Introduction

Numerous aqueous-borne coatings are designed around a polymeric base which is prepared by radical polymerization in emulsion.[1,2] Despite their environmental friendliness, aqueous-borne coatings have not entirely supplanted solvent-borne coatings because of the high hydrophilicity of the intrinsic constituents of the polymer (acrylates, vinyl acetate, etc.). The preparation of hydrophobic and durable aqueous-base coatings would be highly desirable. We[3−8] and Mecking[9−14] have separately reported the possibility of polymerizing ethylene (E) in emulsion via a catalytic pathway. Latexes of high-density polyethylene (HDPE) were prepared, but such products, which are essentially crystalline, could not form films when the latex was applied on a substrate. This spiked our interest in investigating the preparation of less crystalline E-rich copolymers, which are expected to have a lower melting point (T_m) and a glass transition temperature (T_g) higher than the one of PE.[15] For example, we recently demonstrated that it is possible to prepare coatings with moderate anticorrosion properties using copolymers of norbornene and ethylene.[15,16] We also have shown that the catalytic copolymerization of ethylene with polar comonomers such as *N*-vinylpyrrolidone and *N*-isopropylacrylamide yields materials which are wettable by water.[17] On the basis of these past results, it is expected that the preparation of latexes composed of copolymers of ethylene and acrylic monomers would combine the best of two worlds: the exceptional durability, hydrophobicity, and imperviousness to environmental damage of polyolefins to the myriad of benefits of polyacrylates such as high UV stability, adhesive properties, and polarity, to list just a few. For the first time, we report the preparation of such material using the catalytic copolymerization of E and acrylates such as methyl acrylate (MA), *n*-butyl acrylate (BA), benzyl acrylate (BnA), and 2-phenoxyethyl acrylate (PEA) in emulsion.

*Corresponding author. E-mail: claverie.jerome@uqam.ca.

The catalytic copolymerization of ethylene (E) and acrylates has only been explored recently. Brookhart et al. discovered that cationic palladium diimines can copolymerize ethylene and acrylates to afford branched copolymers.[18] The acrylate is placed in an end-chain position through a chain walking reaction. On the basis of this mechanism, Popeney et al.[19] reported that it is possible to prepare copolymers with high levels of acrylate incorporation using cyclophane-based Pd(II) *N,N*-α-diimine complexes where the axial binding sites are shielded. Drent et al.[20] recently disclosed that an ill-defined catalytic system containing a phosphine sulfonate and a palladium complex (tris(dibenzylideneacetone)dipalladium(0) ($Pd_2(dba)_3$) or palladium(II) acetate ($Pd(OAc)_2$)) permits the copolymerization of ethylene and acrylates where the acrylates are incorporated in a main-chain position. Well-defined palladium catalysts containing a phosphine aryl sulfonate ligand were then disclosed by Hearley et al.,[21] Goodall et al.,[22,23] Kochi et al.,[24,25] Liu et al.,[26] Skupov et al.,[27] Luo et al.,[28] Borkar et al.[29] and Vela et al.[30] Among those reports, acrylate copolymerization with ethylene was only mentioned by Goodall,[22,23] Skupov,[27] and Kochi.[24] During the elaboration of this paper, it was recently reported that using a palladium aryl sulfonate catalyst ligated by DMSO instead of pyridine, it was possible to attain very high acrylate incorporations with the possibility of homopolymerizing an acrylate.[31]

2. Experimental Section

1. Materials. All manipulations were done under argon using standard Schlenk techniques. Ligands **1a** (2-[bis(2-methoxyphenyl)-phosphanyl]-4-methylbenzenesulfonic acid and **1b** (2-[bis(2-methoxyphenyl)phosphanyl]benzenesulfonic acid were prepared according to published procedures.[22,32] Catalysts **2a** and **2b** were prepared and characterized according to the literature.[27] Solvents were purified by distillation over CaH_2 and degassed using three freeze−pump−thaw cycles and kept over activated molecular sieves. Water was ultrapure grade (18.2 MΩ) and degassed by boiling for 120 min, followed by sparging with Ar for several hours. All acrylic monomers were purified by sparging them with argon and passing it

Published on Web 08/24/2009

over a bed of inhibitor remover resin (Aldrich). They were then spiked with *tert*-butyl catechol (0.25% w:w). Sodium dodecyl sulfate (SDS) was recrystallized from methanol.

2. Polymerization Procedures. Depending on the volume of solvent and the reaction pressure, polymerizations were carried out in a stainless steel reactor (450 mL, Parr) for pressures comprised between 80 and 400 psi or in Andrews Glass Labcrest glass pressure reaction bottle (150 mL) for pressures comprised between 15 and 100 psi.

2.1. Typical Polymerization in Organic Solution. In a Schlenk flask, 6.6 mg (16.4×10^{-6} mol) of ligand **1b** and 6.0 mg (6.56×10^{-6} mol) of tris(dibenzylideneacetone)dipalladium ($Pd_2(dba)_3$) were dissolved in 100 mL of toluene containing 1 g of methyl acrylate and 1 mg of 2,6-di-*tert*-butyl-4-methylphenol (BHT). This solution was then introduced in a stainless steel reactor which was immediately pressurized with 100 psi ethylene and heated at 100 °C. When this temperature was reached, the pressure was raised to 300 psi and maintained constant throughout the experiment. The activities were calculated from the rate of ethylene consumption which was monitored by the decrease of the ethylene pressure in the feed tank. The pressure in the feed tank was digitally recorded (1 point every 0.1 s), and the loss of pressure was converted into the number of moles of ethylene consumed over time. The TOF was calculated as the time derivative of this number divided by the number of moles of catalyst. After 1 h, the reactor was cooled down to room temperature and slowly depressurized. The polymers were precipitated in four volumes of methanol, collected by centrifugation or filtered, washed with methanol, and dried under vacuum.

2.2. Typical Polymerization in Emulsion. Catalyst **2a** (35 mg) was dissolved in 2.5 mL of dichloromethane containing 0.5 g of hexadecane and 2 mg of BHT in a Schlenk flask. This solution was added by cannula transfer to 50 mL of an aqueous solution of sodium dodecyl sulfate, SDS (concentration 15 g/L), containing 2 mg of 4-hydroxy-2,2,6,6-tetramethylpiperidin-1-oxyl (hydroxyTEMPO). The mixture was sonicated using a 600 W Branson sonicator for 4 min and then introduced into pressure reactor. The reactor was then loaded with 2 g of methyl acrylate and pressurized with ethylene. Activities (TOF) were recorded in the same manner as for solution experiments. After several hours (100 °C, 1000 rpm), the reaction was stopped, and a free-flowing white latex was collected from the reactor.

3. Characterization. The molecular weight distributions were determined by gel permeation chromatography (GPC) using a Viscotek HT GPC equipped with triple detection operating at 160 °C. The eluent was 1,2,4-trichlorobenzene, and separation was performed on three PolymerLabs Mixed B(-LS) columns. The dn/dc of pure linear polyethylene was found to be 0.106 mL/g at this temperature. The dn/dc of several copolymers was also determined. A linear extrapolation between the dn/dc of the copolymer and the wt % composition in acrylate was then performed, leading to the determination of an extrapolated dn/dc of a poly(methyl acrylate) (0.2179 mL/g). The dn/dc of any copolymer was then calculated as the weighted-average of the dn/dc of pure PE and dn/dc of pure poly(methyl acrylate). Particle sizes were measured by quasi-elastic light scattering (QELS) on a light-scattering Microtrac VSR S3000. Transmission electron microscopy (TEM) measurements were effected on a Tecnai12 (V = 80 or 120 kV, W filament) using uranyl acetate as negative contrast agent and a Morada 13MPX digital camera. Samples were first ultrafiltered for serum exchange and then lightly sonicated before applying on the TEM grid. All the NMR spectra were recorded on Varian 400 MHz (Mercury) and 500 MHz (Inova). NMR spectra of the polymers were recorded in d_4-*o*-dichlorobenzene (ODCB) at 115 °C.

4. Variable Temperature NMR Experiments. These studies were performed by recording ^{1}H NMR and ^{13}C NMR spectra of catalyst **2b** in dichloromethane-d_2 (c = 0.104 mol/L) with various amounts of pyridine and monomers at temperatures ranging from −90 to −60 °C. The temperature of the spectrometer was calibrated using the standard MeOH calibration technique. Actual temperatures can be obtained using the following regression: actual temperature = nominal temperature × 1.0435 + 0.8442. Once the spectra were recorded, they were analyzed using the Mexico program by Bain for exchange processes.[33] Pyridine was set as a AA′BB′C system.[34] The Mexico program relies on the knowledge of the line width and chemical shifts of bound and free pyridine in the absence of exchange. The line width of free pyridine in the absence of exchange (i.e., the absence of catalyst) was measured at −90 °C. The same line width was used for pyridine bound to the catalyst. The variation of the chemical shifts of pyridine with temperature was also taken into account by recording the spectrum of pyridine and of the catalyst alone at temperatures ranging from −90 to −50 °C. The results generated by the Mexico program were visually checked using WinDNMR software by Reich, which offers the capability to superimpose an experimental spectrum and an exchange simulated spectrum.[35]

Scheme 1. Catalytic Copolymerization of Ethylene with Acrylate

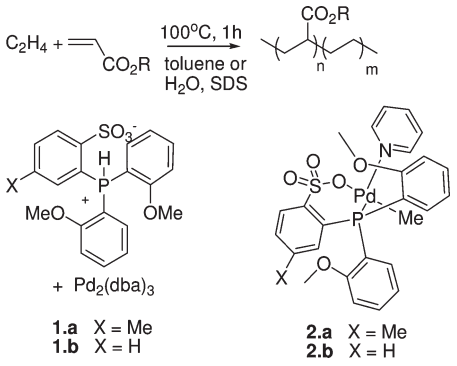

3. Results and Discussion

1. Copolymerization of C_2H_4 and Methyl Acrylate (MA) in Toluene. Drent has reported that it is possible to copolymerize C_2H_4 with MA using in situ formed diarylphosphinobenzene-2-sulfonic acid (**1b**) and $Pd_2(dba)_3$ or $Pd(OAc)_2$.[20] We later reported the synthesis of the corresponding neutral catalyst for the copolymerization of C_2H_4 and acrylates by reaction of diarylphosphinobenzene-2-sulfonic acid with $PdMe_2$(tmeda) in the presence of pyridine (**2a** and **2b**, Scheme 1).[27]

These catalysts are active for the copolymerization of various acrylates with C_2H_4. The instantaneous activities or turnover frequencies (TOF) in moles of C_2H_4 per mole of palladium and per hour reported in this paper correspond to the rate at which ethylene is consumed from a feed tank. The TOF values reported in Table 1 are the maximum activity values once the reactor has reached its set-point temperature and once the dissolution of ethylene is over. In our experimental setup, heating and dissolution last for ∼15 min, and the kinetics curves (Figure 1) start after this initial 15 min delay is passed. These values are reproducible (less than 10% deviation between repeat experiments) as long as the same reactor and the same experimental parameters (stirring, stirrer design, cooling loop design, temperature of the cooling liquid, etc.) are used. When the catalytic activity is low, such as in the case of emulsion reactions, these TOF values can be difficult to measure because the pool of dissolved ethylene initially present in the reaction solvent is sufficient to supply the catalyst during the reaction. Turnover numbers (TON) for C_2H_4 and MA are also reported in this paper. The TON value corresponds to the total amount in moles of C_2H_4 (or of MA) inserted per mole of catalyst divided by the reaction time. This number, calculated from the copolymer

Table 1. Copolymerization of C_2H_4 with Various Acrylates (MA: Methyl Acrylate; BA: *n*-Butyl Acrylate; BnA: Benzyl Acrylate; PEA: 2-Phenoxyethyl Acrylate)

expt[a]	T (°C)	cat.[h]	mon	[mon] (g/L)	P (psi)	pol wt (g)	SC[b] (%)	dp[c] (nm)	M_n[d] (g/mol)	%A[e]	TOF (h^{-1})	TON (C_2H_4), h^{-1}	TON (A), h^{-1}
1S	100	**1b**	MA	100	300	0.6			5400	6.9	600	735	110
2S	100	**2b**	MA	100	300	1.4			9800	6.3	1800	1605	320
3S	100	**1b**	MA	50	200	0.4			nd	6.4	< 500	540	75
4S	100	**1a**	MA	50	200	0.35			nd	5.6	< 500	350	40
5S	115	**2b**	MA	10	300	3.0			5900	1.1	4050	4715	105
6S	85	**2b**	MA	10	300	2.5			21000	0.6	2650	3180	40
7S	100	**2b**	MA	10	300	4.0			5800	0.8	5300	6380	100
8S	100	**2b**	MA	10	100	0.65			8900	2.6	900	960	50
9S	100	**1a**	MA	10	100	0.85			9500	2.6	870	1030	55
10S	100	**1a**	MA	10	200	1.0			11600	1.5	720	1580	50
11S	100	**1a**	MA	10	300	2.35			13400	1.0	3400	3730	75
12S	100	**2b**	MA	40	60	0.10			nd	9.6	42	55	11
13S	100	**1b**[f]	MA	25	60	0.13			nd	6.8	200	48	4
14S	100	**1b**[f]	MA	25	100	0.40			2200	6.6	526	146	11
15S	100	**1b**[f]	BA	35	60	0.04			nd	6.3	54	13	1
1E[g]	100	**1b**	MA	40	60		floc	floc	nd	nd	nd	nd	nd
2E[g]	100	**2a**	MA	200	90		floc	floc	nd	nd	nd	nd	nd
3E	100	**2b**	MA	40	50		4.5	185	5400	2.7	nd	420	8
4E	100	**2b**	MA	40	50		5.0	135	15000	2.8	nd	36	0.7
5E	100	**2a**	MA	140	85		0.9	678	5000	1.2	nd	13	0.1
6E	100	**2b**	MA	40	65		1.9	197	4500	1.0	nd	136	0.9
7E	100	**2b**	BnA	60	60		3.6	209	nd	9.7	nd	154	25
8E	100	**2b**	BA	60	300		2.2	108	nd	3.4	nd	519	27
9E	100	**2b**	PEA	100	70		1.8	170	nd	8.1	nd	110	14

[a] S: polymerization in toluene; E: polymerization in emulsion. [b] Solid content of the latex determined by gravimetry. [c] Particle diameter by DLS. [d] Determined by GPC (not suitable when the weight of polymer is less than 0.4 g). [e] Molar incorporation of acrylate determined by ^{1}H NMR. [f] $PdMe_2(tmeda)$ was used as a source of Pd. [g] No hexadecane and no sonication were used for this experiment. [h] For the ligands **1a** and **1b**, $Pd_2(dba)_3$ was used as source of Pd.

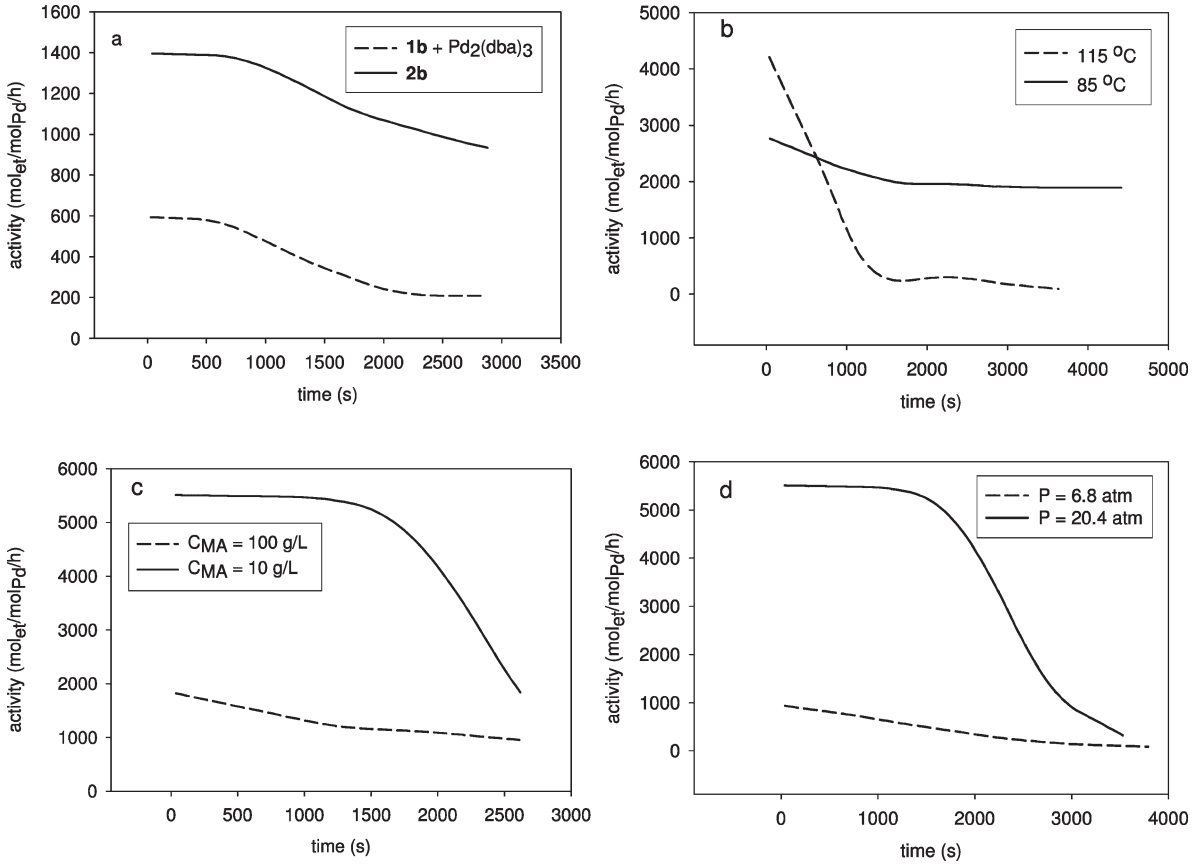

Figure 1. Influence of reactions parameters on the activity of the catalyst. (a) Influence of the nature of the catalyst: **1a** + $Pd_2(dba)_3$ (dashed line, expt 1S) vs **2b** (solid line, expt 2S) ([Pd] = 110 μmol/L, [MA] = 100 g/L, T = 100 °C, $P(C_2H_4)$ = 300 psi). (b) Influence of temperature: T = 115 °C (dashed line, expt 5S) vs T = 85 °C (solid line, expt 6S) ([**2b**] = 110 μmol/L, $P(C_2H_4)$ = 300 psi, [MA] = 10 g/L). (c) Influence of MA concentration: [MA] = 100 g/L (dashed line, expt 2S) vs [MA] = 10 g/L (solid line, expt 7S) ([**2b**] = 110 μmol/L, T = 100 °C, $P(C_2H_4)$ = 100 psi). (d) Influence of ethylene pressure: $P(C_2H_4)$ = 100 psi (dashed line, expt 8S) vs $P(C_2H_4)$ = 300 psi (solid line, expt 7S) ([**2b**] = 110 μmol/L, T = 100 °C, [MA] = 10 g/L).

yield and composition, is accurate even for low activity reactions but is influenced by both the rate of monomer insertion and the rate at which the catalyst is deactivated. Hence, this TON value should not be used to extract kinetic information.

Only experiments where temperature was controlled (exotherm less than 5 °C) are reported here. Consequently, experiments where large amounts of catalyst were used, which in our hands lead to higher acrylate incorporations, were not included in this study.

In the case of homopolymerization of C_2H_4, the activities of the in situ and well-defined systems are comparable.[27] However, for the copolymerization of C_2H_4 with MA, the activity of the in situ system is 2−3 times lower than for the well-defined catalyst (Figure 1a, Table 1, experiments 1S and 2S), seemingly indicating that a lower number of sites are active for the in situ system. Comonomer incorporations are similar for copolymerizations ran with both systems. Ligand **1b**, based on a benzenesulfonic acid backbone, is similar in terms of catalytic activity, molecular weight, and comonomer incorporation to ligand **1a** based on *p*-toluenesulfonic acid (Table 1, comparing experiments 3S and 4S). In our hands, it was slightly easier to dehydrate benzenesulfonic acid than toluenesulfonic acid, allowing the synthesis of **1b** to proceed with a higher yield than for **1a**.[22] The use of either structure **a** (toluenesulfonic) or **b** (benzenesulfonic) does not offer any significant advantage or difference, and both catalysts will be used interchangeably in the rest of the discussion.

The copolymerization can be performed at temperatures ranging from 85 to 110 °C. As expected (Figure 1b), the catalytic system has a shorter lifetime (less than 1 h) and a higher maximum activity (TOF) at 110 °C. This TOF value is likely underestimated because a significant portion of the catalyst is deactivated before the temperature of 110 °C is reached. At 85 °C, the polymerization can be sustained for several hours with a low activity. An acceptable compromise is around 100 °C, maximizing activity and productivity. As expected, the molecular weights of the copolymer decrease with increasing reaction temperature (compare experiments 5S, 6S, and 7S). For all copolymers, main-chain incorporation of the acrylate has been demonstrated by ^{1}H NMR analysis: for every methyne C**H**−CO(OMe) proton, four methylene protons −C**H**$_2$−CHCO(OMe)−C**H**$_2$− are observed in two separate peaks corresponding to the two diastereotopic positions. Polymers are also linear (as demonstrated by Mark−Houwink plots in GPC and by NMR). Polymers for which the chain ends could be detected by ^{1}H NMR were terminated by the usual β-hydride elimination process, occurring either after an ethylene (>75%) or after a 2,1-acrylate insertion (<25%). The activity depends on the concentration of both comonomers (Figure 1c,d), indicating that the polymerization kinetics is not zero order with respect to monomer concentration (see below).

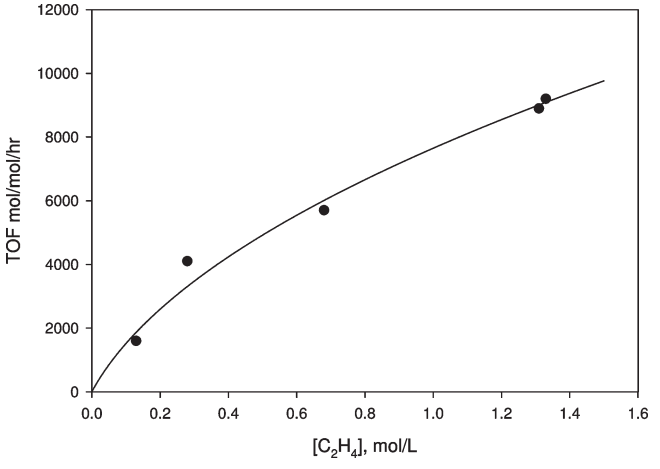

Figure 2. Activity vs C_2H_4 concentration for C_2H_4 homopolymerization by catalyst **2b** (see experimental conditions in Table 2). The solid-line curve is a fit of the activity TOF vs concentration of ethylene using $k_2 = \mathrm{TOF}_{max} = 102\ s^{-1}$, $k_1 = 5\ L\ mol^{-1}\ s^{-1}$, and $k_{-1} = 10^8\ L\ mol^{-1}\ s^{-1}$ (details on the fit given in the Supporting Information).

The kinetics of homopolymerization of ethylene can be seen as an equilibrium between coordination and dissociation of C_2H_4 on the active site and insertion of C_2H_4 in the Pd−alkyl bond (Scheme 2).

In order to determine k_2, k_{-1}, and k_1, the following approach was adopted. First, analytical expressions for the concentration of pyridine and for TOF were determined (see Supporting Information). Initial guesses for k_2, k_1, and k_{-1} were chosen, allowing us to calculate a TOF value which could be compared to experimentally measured TOF. These kinetic constants were then adjusted by a nonlinear optimization procedure until the error between calculated and experimental TOF was minimal. The best-fit values of k_2, k_1 and k_{-1}, were found to be respectively 102 s^{-1}, 5 L mol^{-1} s^{-1}, and 10^8 L mol^{-1} s^{-1}. Although there is a good agreement between measured and calculated TOF values (Table 2 and Figure 2), the accuracy is probably low due to the limited number of experimental data. Notwithstanding the exact values of these rate constants, it is possible to draw several conclusions based on their order of magnitude. First, the pyridine coordination equilibrium is very much in favor of the pyridine bound form ($K = k_1/k_{-1} \sim 10^{-7}$). Second, the activity is maximum when all the Pd are bound to C_2H_4, that is to say, when the rate of polymerization is $k_2[\mathrm{Pd}]_0$ and therefore when the turnover frequency is $\mathrm{TOF}_{max} = k_2$. The ratio of the measured activity TOF to the maximum activity, TOF_{max}, is the proportion of Pd atoms that are coordinated to C_2H_4. At a pressure of 300 psi, only 3% of the catalyst is bound to C_2H_4 and 97% bonded to pyridine at a given time (Table 2). Although the conditions are very different (catalyst concentration higher and C_2H_4 pressure lower in the NMR tube), it will be seen below that C_2H_4 bound Pd species are not observed spectroscopically, which is also indicative of an unfavorable pyridine substitution by C_2H_4. Last, under polymerization conditions, the reaction of C_2H_4 coordination ($R_1 = k_1[C_2H_4][\text{Pd-pyr}]$, Table 2) goes approximately at the same rate than the insertion reaction ($R_2 = k_2[\text{Pd}-C_2H_4]$). Contrarily to our initial belief, the insertion step is not preceded by a fast pre-equilibrium of ethylene coordination: both reactions go at comparable rates. Thus, the palladium will exchange pyridine by C_2H_4 and inversely only a few times (on average twice) before insertion occurs.

Scheme 2. Kinetic Scheme for C_2H_4 Homopolymerization

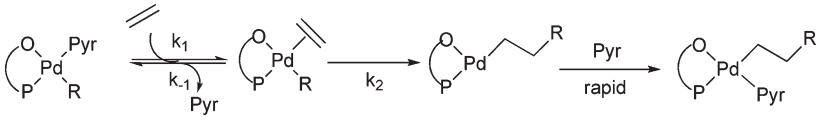

Table 2. Influence of the C_2H_4 Pressure for C_2H_4 Homopolymerization with Catalyst 2b[a]

pressure C_2H_4 (psi)	$[C_2H_4]$[b] (mol L^{-1})	TOF (mol mol^{-1} h^{-1})	% pyridine bound[c]	% C_2H_4 bound[c]	R_1[d] (mol L^{-1} s^{-1})	R_2[e] (mol L^{-1} s^{-1})
47	0.13	1600	99.5	0.5	5.4×10^{-5}	3.9×10^{-5}
90	0.28	4100	99	1	1.2×10^{-4}	7.0×10^{-5}
200	0.68	5700	98	2	2.8×10^{-4}	1.3×10^{-4}
257	1.31	8900	97	3	5.4×10^{-4}	1.9×10^{-4}
287	1.33	9200	97	3	5.4×10^{-4}	1.9×10^{-4}

[a] All reactions were performed with a catalyst concentration of 76 μmol/L in 50 mL toluene at 85 °C (reactor size: 100 mL). [b] Concentration of C_2H_4 in saturated toluene calculated using Peng−Robinson thermodynamic state equations for toluene and ethylene (data not shown). [c] Calculated from the ratio of TOF to TOF_{max}, using the calculated value of $k_2 = 102\ s^{-1}$ for TOF_{max} (= 368 000 mol mol^{-1} h^{-1}). [d] Calculated rate of the C_2H_4 coordination reaction (forward rate). [e] Calculated rate of the insertion reaction. The concentrations of Pd bound to ethylene and palladium bound to pyridine were calculated using equations developed in the Supporting Information.

Table 3. Influence of Various Additives on C_2H_4 Homopolymerization by 2 and 3

solvent	temp (°C)	$P(C_2H_4)$ (psi)	[catalyst] (μmol/L)	TOF (mol mol^{-1} h^{-1})
		Catalyst **3**		
toluene	100	300	5	570×10^3
toluene + 5 mL of EtOAc	100	300	5	86×10^3
THF	85	300	5	16.7×10^3
THF + 0.2 mL of water	85	300	5	14.8×10^3
THF + 1 mL of water	85	300	5	13.8×10^3
THF + 5 mL of water	85	300	5	10.5×10^3
THF + 10 mL of water	85	300	5	9.1×10^3
		Catalyst **2b**		
EtOAc	100	300	51	740
methyl propionate	100	300	51	530
toluene[a]	100	380	104	8900
toluene + 6 mL of EtOAc[a]	100	380	104	6800

[a] Copolymerization with MA (10 g/L).

In the case of C_2H_4 and MA copolymerization, the kinetic scheme includes two pyridine displacement reactions (one by MA, the other one by C_2H_4) and four possible propagation steps (insertion of MA and C_2H_4 in a C_2H_4 or a MA terminated growing chain). Moreover, the oxygen lone pair of the carbonyl group of the acrylate could coordinate the catalyst: in this case, MA would not only be a monomer but also an inhibitor of the catalyst. Consequently, all copolymerizations are characterized by a significant decrease in activity; however, Guironnet et al.[31] have rather concluded that this decrease was due to a slow insertion of monomer in [(PO)Pd{CH(COOMe)CH_2R}(monomer)]. On the basis of the pioneering work of Brookhart et al. on cationic palladium diimines,[36] Drent et al.[20] have inferred that the decrease of activity was due to the formation of a stable chelate after acrylate insertion.

To clarify which phenomenon is responsible for the loss of catalytic activity in C_2H_4 and MA copolymerizations, polymerizations were performed in the presence of a nonpolymerizable ester analogue to MA such as ethyl acetate and methyl propionate (Table 3). Compared to polymerizations ran in toluene, the use of an ester as solvent results in lower activities. This indicates that esters have the capability to coordinate the catalyst. This was also confirmed for catalyst **3**[27] (Scheme 3), which has a high activity but only inserts very small amounts of acrylates (Table 3). The addition of 5% ethyl acetate in the solvent results in a 7-fold decrease in catalytic activity, clearly indicating that esters inhibit the catalyst (the solubilities of the catalyst and of ethylene are not expected to be drastically changed by the addition of 5% of ethyl acetate). The "poisoning" effect of ethyl acetate was also noticeable during the copolymerization of acrylates (Table 3): the copolymerization rate is decreased by 30% when ethyl acetate at a concentration of 35 g/L is present.

Scheme 3. Catalyst 3 Structure

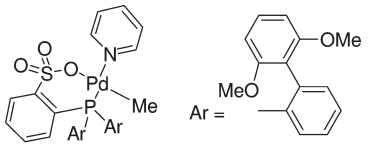

3

Before embarking upon the determination of the rate of the substitution of pyridine by an acrylate (or more generally by an ester), a simpler reaction of pyridine exchange was studied (Scheme 4). The exchange kinetics of pyridine in either bound or free states has been studied in dichloromethane by both ^1H and ^{13}C NMR line shape analysis over a wide range of temperatures.[37] At room temperature, a sample of catalyst **2b** containing 3% free pyridine exhibits two separate set of resonances for the pyridine protons in ^1H NMR at room temperature (Figure 3a), whereas only a single time-averaged resonance is observed when 10% free pyridine is added (Figure 3b). Using a procedure which has been extensively used for the study of supramolecular processes, the resonance of each time-averaged peak, either in a slow-exchange regime or in fast-exchange regime, can be fitted by a Lorentzian, whose shape is dependent on a parameter τ defined as the lifetime of pyridine interaction (Figure 4).[38] This lifetime is defined mathematically as $\tau_A\tau_B/(\tau_A + \tau_B)$, where τ_A and τ_B are respectively the lifetime of pyridine in the bound and free state.[38] This experiment was performed at various temperatures and for three different concentrations of added pyridine. The resonance of the CH=N proton was analyzed both by ^{13}C and ^1H NMR, leading to two values of τ which were averaged in Table 4.

For Scheme 4, the lifetime τ is given by[37−39]

$$\frac{1}{\tau[\text{pyridine}]_{\text{total}}} = k_1 + k_2 \frac{1}{[\text{pyridine}]_{\text{free}}} \qquad (1)$$

Hence, a plot of $1/(\tau[\text{pyridine}]_{\text{total}})$ vs $1/[\text{pyridine}]_{\text{free}}$ should yield a straight line of slope k_2 (rate constant of the exchange reaction by a dissociative mechanism) and intercept k_1 (rate constant of the exchange reaction by an associative mechanism).

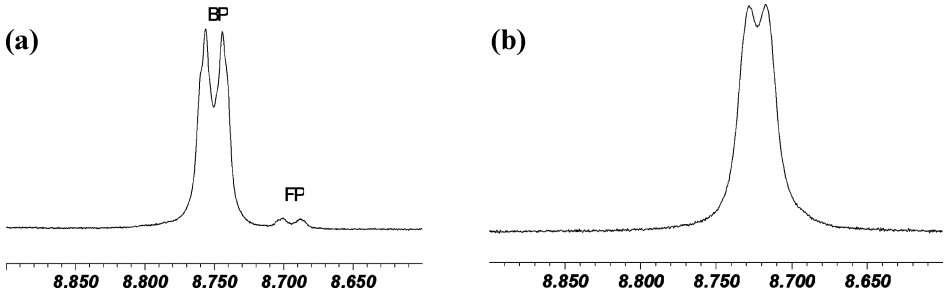

Figure 3. Resonance of the proton α to nitrogen in pyridine for catalyst **2a** in CD_2Cl_2 at room temperature. BP: bound pyridine; FP: free pyridine. (a) Slow exchange regime (catalyst **2a** + 3% pyridine). (b) Fast exchange regime (catalyst **2a** + 10% pyridine).

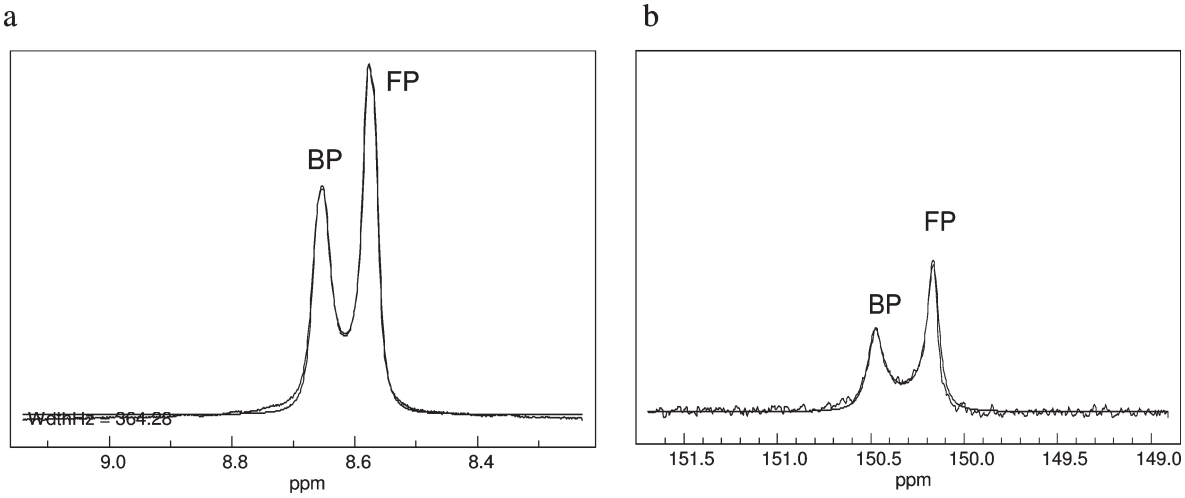

Figure 4. Overlay of the calculated and experimental ^1H NMR (a, left) and ^{13}C NMR spectra (b, right) for catalyst **2a** (0.079 mol/L) and added pyridine (0.104 mol/L) in CD_2Cl_2 at −90 °C.

Scheme 4. Possible Mechanisms for Pyridine Exchange

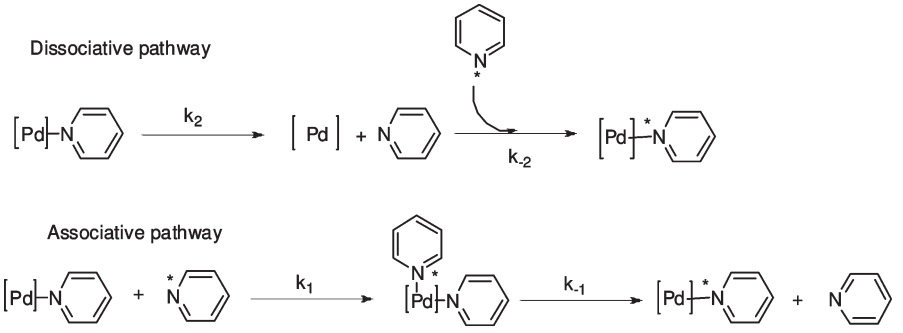

Figure 5 clearly indicates that at temperatures ranging from −90 to −60 °C the dissociative contribution (slope) is negligible, and pyridine exchange occurs exclusively by an associative pathway. Higher temperatures cannot be probed with this technique because the fast exchange limit is reached, except when minuscule concentrations of FP are used (see Figure 3a). An Eyring plot (Figure 6) indicates that the activation parameters for the associative exchange are $\Delta H^{\ddagger} = 16.8$ kJ/mol and $\Delta S^{\ddagger} = -98$ J mol^{-1} K^{-1}, the negative value for the activation entropy being expected for an associative process.

We now turn our attention toward the displacement of pyridine either by an acrylate or by C_2H_4. On the basis of the fact that pyridine exchange occurs by an associative mechanism, we assume that the substitution of pyridine by MA or by C_2H_4 also occurs via an associative route (Scheme 5). This substitution reaction occurs at a time scale which can be probed by NMR, as shown in Figure 7: the resonances of the pyridine protons coalesce in the presence of MA or ethylene. It is important to state that neither acrylate nor ethylene-bound complexes are observed spectroscopically, indicating that pyridine is a stronger donor. However, the presence of either MA or ethylene is decreasing the interaction lifetime of pyridine τ, as observed by NMR.

Neglecting the dissociative component of the mechanism, this lifetime is given by

$$\frac{1}{\tau} = k_1[\text{pyridine}]_{\text{total}} + k_{1X}[X]_{\text{total}} \qquad (2)$$

Table 4. $1/\tau$ for Catalyst 2a in CD_2Cl_2 at Temperatures Ranging from −60 to −90 °C (BP: Bound Pyridine: FP: Free Pyridine)[a]

$1/\tau$ (s^{-1})	[BP] (mol/L)	[FP] (mol/L)
	temperature = −60 °C	
321	0.079	0.105
266	0.024	0.086
285	0.079	0.052
197	0.073	0.034
	temperature = −70 °C	
195	0.079	0.105
124	0.024	0.086
178	0.079	0.052
123	0.073	0.034
	temperature = −80 °C	
112	0.079	0.105
74	0.024	0.086
106	0.079	0.052
74	0.073	0.034
	temperature = −90 °C	
61	0.079	0.105
42	0.024	0.086
59	0.079	0.052
42	0.073	0.034

[a] Above −60 °C, coalescence has occurred and the width of the peak is principally influenced by experiment-dependent parameters ($1/T_2$*) and not by the exchange process.

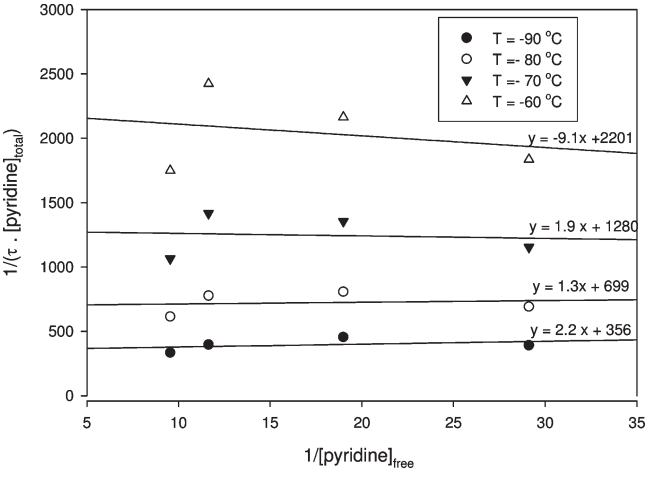

Figure 5. Plot of $1/(\tau[\text{pyridine}]_{\text{total}})$ vs 1/[pyridine] for catalyst **2a** in CD_2Cl_2.

Using both ^1H and ^{13}C NMR line shape analysis, τ was measured at several temperatures (Table 5). The values of k_1 were calculated from the activation parameters obtained above (Figure 6). From eq 2, the kinetic rate constant for ligand displacement, k_{1X}, can thus be obtained. However, for the case of susbstitution of pyridine by C_2H_4, the C_2H_4 concentration dissolved in the sample changes considerably with temperature, and no reliable values could be obtained for k_{1E}. For the associative substitution of pyridine by MA, it was found that the activation parameters are $\Delta H^{\ddagger} = 18.1$ kJ/mol and $\Delta S^{\ddagger} = -87$ J mol^{-1} K^{-1} (Figure 6 and Table 5).

Importantly, using this technique, it is not possible to assess whether the activation parameters measured for acrylate coordination correspond to coordination via a π-bond (involving the C=C) or via a σ-bond (involving the O lone pair). Interestingly, the activation parameters for pyridine or

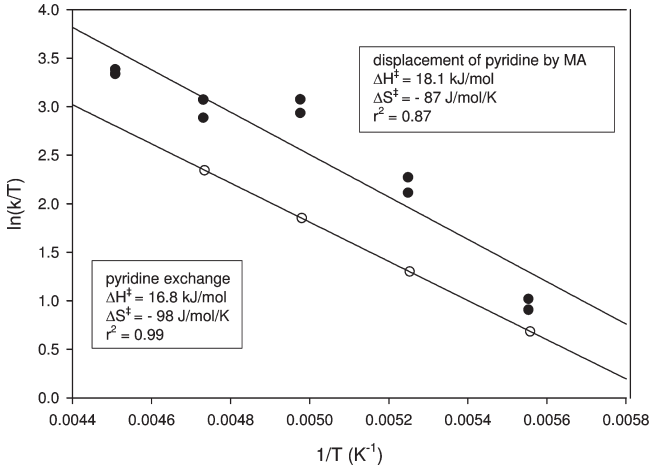

Figure 6. Eyring plots for the substitution of pyridine by pyridine and by MA via an associative mechanism.

MA coordination on the catalyst are significantly smaller than the literature values reported for olefin complexation on other late transition metal polymerization catalysts. For example, the activation enthalpies of complexation of C_2H_4 on salicylaldiminato nickel or cationic palladium diimines complexes have been calculated to be in the range of 50−80 kJ/mol.[40,41] However, to our knowledge, these energies have been calculated by removing the phosphine ligand to produce a coordinately unsaturated site followed by coordination of ethylene. Therefore, a dissociative process has been implicitly assumed by the authors, whereas in our case an associative pathway is taking place. For our catalysts, the low enthalpy of activation is balanced by the very negative activation entropy consistent with an associative process.

To conclude on this section, it is clear that the displacement of pyridine by C_2H_4 or acrylate is a key step in our polymerizations. Removal of pyridine would have for effect to transfer the limiting step toward olefin insertion for ethylene polymerization. This was achieved by Guironnet et al.[31] with the preparation of a DMSO-ligated sulfonated arylphosphine palladium complex. Vela et al.[30] have also shown that pyridine can be captured with tris(pentafluorophenyl)borane, generating a catalyst that is more active for polymerization of ethylene. However, even when pyridine is removed or absent, the catalyst is poisoned by σ-coordination of the acrylate.

2. Emulsion Copolymerization of C_2H_4 and Acrylates. Catalysts **2a** and **2b** have been shown to promote the emulsion copolymerization of C_2H_4 with styrene[29] and with norbornene.[15] The results of MA-E copolymerization in organic solution encouraged us to probe an emulsion polymerization process with the aim of latex formation. In our hands, the copolymerization of E and an acrylate by the system $Pd_2(dba)_3$**/1a** or **1b** (expt 1E, Table 1) generates polymer particles with large sizes ($\gg 1$ μm), unlike an emulsion polymerization which yields nanoparticles. Therefore, all emulsion polymerizations were performed with the well-defined catalysts **2a** and **2b**. When **2a** or **2b**, dissolved in a small amount of organic solvent, is added to water and surfactant, the polymerization reaction results in the formation of millimeter size polymer particles (expt 2E, Table 1). However, the final product of the reaction is a latex when the initial organic solution containing **2a** or **2b** is miniemulsified, that is to say, when o/w nanosize droplets are formed upon sonication of an emulsion containing the organic solution, hexadecane, water, and surfactant. Attempts to bypass this emulsification procedure results either in the formation of

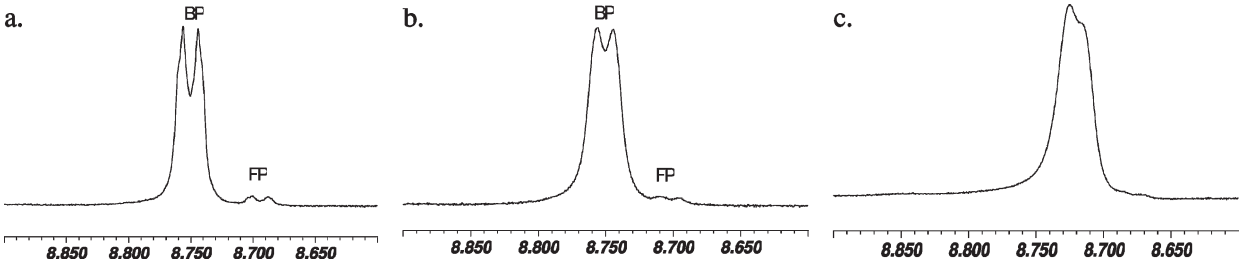

Figure 7. Resonance of the proton α to nitrogen in pyridine for catalyst **2a** in CD_2Cl_2 at room temperature. BP: bound pyridine; FP: free pyridine. (a) Catalyst **2a** with 3% of FP. (b) Catalyst **2a** with 3% of FP and 5 equiv of ethylene. (c) Catalyst **2a** with 3% of FP and 1 equiv of MA.

Table 5. $1/\tau$ for Catalyst 2a in CD_2Cl_2 at Temperatures Ranging from −50 to −90 °C, Obtained by Line Shape Analysis of ^1H and ^{13}C Spectra

T (°C)	$1/\tau$ (Hz) (^1H NMR)	$1/\tau$ (Hz) (^{13}C NMR)	$k_1{}^a$ (L mol^{-1} s^{-1})	k_{1A} (L mol^{-1} s^{-1}) (^1H NMR)	k_{1A} (L mol^{-1} s^{-1}) (^{13}C NMR)
−90	32	30	358	445	498
−80	85	95	700	1840	1570
−70	210	189	1281	3780	4340
−60	253	224	2213	3780	4560
−50	369	380	3641	6530	6230

[a] Calculated from the activation parameters of Figure 6.

Scheme 5. Substitution of Pyridine by Ethylene (X = H) or an Acrylate (X = COOR)

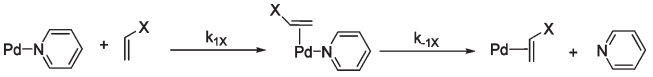

polymers which are not dispersed or in the absence of polymerization (probably because of the poor accessibility of the catalyst in the medium). The miniemulsion droplets have a diameter around 150 nm, as measured by dynamic light scattering. They remain stable for several hours. The role of hexadecane is to prevent Ostwald ripening (disappearance of the smallest droplets and swelling of the largest ones, until the mixture is totally phase separated).[42] The size and stability of this miniemulsion depend on several factors, such as the amount of surfactant and sonication time and power. These parameters are currently under scrutiny in our laboratory. When a miniemulsion is stable, it appears as a homogeneous white medium by optical microscopy (Figure 8a). This is consistent with the fact that the miniemulsion is constituted of droplets smaller than the optical resolution (~1 μm). Then, an acrylate can eventually be added to the aqueous phase. If saturation is reached ($c > 50$ g/L for methyl acrylate, $c < 10$ g/L for all other acrylates), large droplets containing the excess acrylate are formed (Figure 8b, size ≫1 μm). These droplets are significantly larger than the miniemulsion droplets, and they serve as monomer reservoirs during the reaction. No polymer is formed in these large droplets, as shown by the absence of large particles in the final latex (Figure 8c). The amount of organic solvent (dichloromethane) in these polymerizations is small (typically 7 mL per 100 mL of water). Initially, the organic solvent is located in the miniemulsion droplets (size around 150 nm). The reactions are performed at 100 °C, and it is unclear what the proportion of dichloromethane remains in the liquid phase. During the degassing step, we believe that most of the dichloromethane is stripped, yielding a latex virtually free of volatile organic compounds.

With a stable catalytic miniemulsion in hand, the emulsion polymerization can be triggered upon heating in the presence of C_2H_4. At 100 psi and 100 °C, the solubility of C_2H_4 in water has been reported to be ~0.35 g/L, a high enough value to expect its diffusion through the aqueous phase not to be rate-limiting.[43] However, transport of C_2H_4 at the gas−water interface can be rate-limiting: in our hands, activity of the emulsion polymerization strongly depends on the design of the reactor and type of stirring blade used during the polymerization and of course stirring rate. In all cases, the polymerization occurs significantly slower than for polymerization run in organic medium (vide infra).

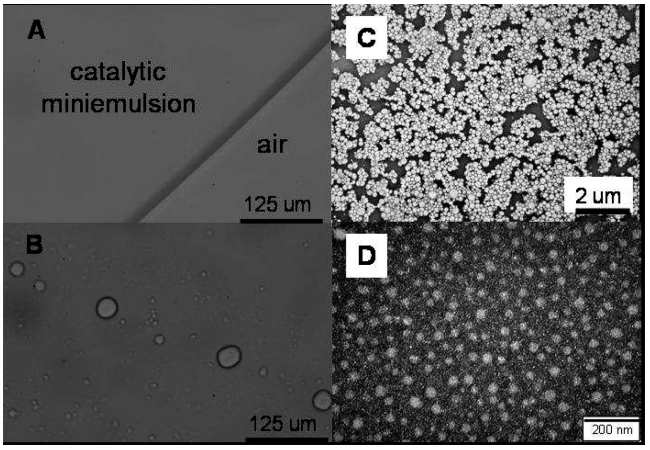

Figure 8. (A) Optical microscopy picture of a catalyst miniemulsion (37 mg of **2** dissolved in 3 mL of CH_2Cl_2 and 0.3 mL of hexadecane dispersed in 100 mL of an SDS aqueous solution, $c = 20$ g/L). The size of the o/w droplets is below optical diffraction limit, resulting in a homogeneous liquid. (B) After adding MA ($c = 100$ g/L) to the catalytic miniemulsion, MA droplets of several micrometers are formed. (C) Transmission electronic microscopy (TEM) picture of the poly(ethylene-*co*-acrylate) nanoparticles formed by polymerization of miniemulsion B (entry 4E of Table 1). (D) TEM picture of the smaller particles ($d = 25 \pm 7$ nm). These particles appear as faint white spots in (C).

The latexes resulting from these polymerizations are formed of particles having a bimodal diameter distribution centered on 120 and 25 nm, as confirmed by TEM (Figure 8 C,D) and dynamic light scattering. These suspensions are colloidally stable and are constituted of mostly spherical particles, which contrasts with the elongated particles observed for HDPE latexes.[4,12] This difference can be explained by the low crystallinity of the poly(ethylene-*co*-acrylate) copolymers. The presence of a population of smaller polymer particles (diameter ~ 25 nm) is a consequence of the high amount of surfactant used in our formulations. On the basis

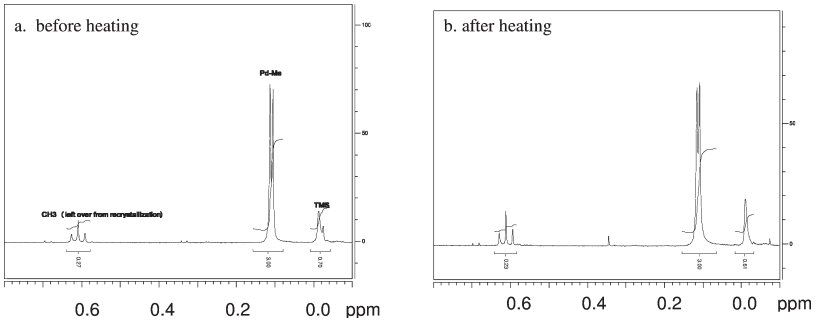

Figure 9. ^{1}H NMR ($C_2Cl_4D_2$) of **2a** (Pd−CH_3 region) after being heated at 100 °C for 2 h in the presence of D_2O (30 mg of **2a** in 1.5 mL of $C_2Cl_4D_2$ and 0.2 mL of D_2O). The inset (Pd−Me region) shows that the methyl group is not degraded under these conditions. No CH_4 (product of hydrolysis of Pd−Me with water, at 0.3 ppm) could be observed.

of the data of Bechthold et al.,[44] the amount of surfactant (SDS) necessary to stabilize droplets of diameter 125 nm is 0.0461 $g_{SDS}/g_{dispersed\ phase}$, whereas an amount of 0.13 $g_{SDS}/g_{dispersed\ phase}$ was used in our case. The excess surfactant forms micelles (initial diameter ∼ 5 nm) which contain catalyst and which are later converted into polymer particles. Therefore, in parallel to the miniemulsion polymerization process, a "microemulsion" polymerization process whereby micelles are nucleated and polymerized is occurring in our reactions.[45]

Interestingly, unlike copolymerizations performed in solutions, latexes made with acrylates such as butyl acrylate, phenoxyethyl acrylate, and benzyl acrylate (BA, PEA, and BnA) have higher acrylate incorporations than those made with MA (expts 7E−10E in Table 1). In the emulsion process, the locus of the polymerization is the growing polymer particle. However, a significant portion of MA is located in the aqueous phase (solubility > 50 g/L) and also in the gas phase at 100 °C, resulting in the formation of polymers with low MA incorporation. By contrast, comonomer incorporations are higher for other acrylates because the polymerization occurs in a polymer particle which only contains polymer, acrylate, C_2H_4, and a trace of organic solvent (at the polymerization pressure and temperature, most of the dichloromethane is in the gas phase). Such experimental conditions would be equivalent to a solution reaction performed in neat monomer.

Spontaneous radical polymerization of the acrylate was only prevented when two radical inhibitors, an organosoluble one (BHT) and a water-soluble one (hydroxyTEMPO), were used. The use of BHT alone was not sufficient to prevent formation of poly(methyl acrylate) via a radical mechanism, which is consistent with the presence of a high concentration of MA in water.

As observed for polymerizations performed in organic solvent, the highest acrylate incorporations in emulsion are reached when the reactions are performed at low ethylene pressure, 50 psi (expts 3E and 4E). The molecular weights of the emulsion polymers are comparable to those obtained in solution if one does not take into account in the GPC chromatogram a very low molecular weight population which was attributed to surfactant and hexadecane.

All the emulsion polymerizations are significantly slower than the solvent ones, resulting in latexes which have low solid contents. Several literature reports have focused on the decrease of activity in the presence of water. DeKock et al. have reported that water promotes the decomposition of the active site via a Wacker-type reaction (attack of HOH on coordinated ethylene).[46] Protonolysis of the metal−alkyl bond (in the absence of ethylene) was also observed for N, O-chelated salicylaldiminate Ni-based complexes (Grubbs catalysts).[47] In our case, the hydrolytic stability of the catalyst was assessed by heating **2a** at 100 °C for several hours in the presence of water (Figure 9): no hydrolysis of the Pd−Me bond was observed.

Scheme 6. Reversible Inhibition of the Catalyst by Water

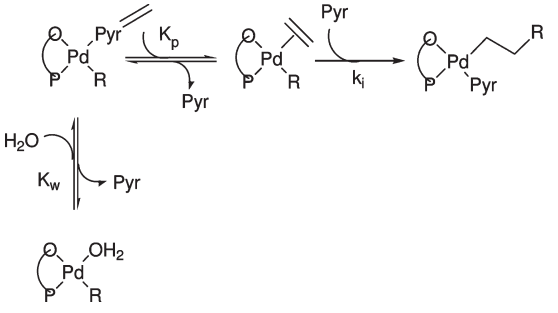

On the basis of the finding that acrylate can coordinate the catalyst in a σ-fashion (vide supra), we have surmised that water may also coordinate the catalyst (Scheme 6). Determination of kinetic parameters in the presence of water for catalysts **2a** and **2b** proved to be difficult because measurements of low activities are not precise with our experimental setup. Therefore, the very active catalyst **3** (Scheme 3) was used for this study. Polymerizations of C_2H_4 were performed in THF containing various concentrations of water, THF being used instead of toluene because it is miscible with water (Table 3). Interestingly, the catalytic activity decreases with increasing concentrations of water (Figure 10), in agreement with the fact that water may coordinate the catalyst. As expected for a competitive inhibitor, there is an inverse relationship between the catalytic activity (TOF) and the concentration of water (Figure 11). For the polymerizations run in anhydrous THF or low concentrations of water, no decrease of the activity over time is observed, which indicates that the catalyst is long-lived under these conditions. When the concentration of water in the system is sufficiently high, a decrease of the activity is observed with time (Figure 10) as some of the active sites have been deactivated by the presence of water. For a water concentration of 3.9 mol/L, the activity after 1 h is 60% of its initial value, indicating that only 40% of the active sites have been decomposed by water. Therefore, the decrease of activity in aqueous medium is due to the combination of two factors: coordination of water on Pd and slow water-induced decomposition of the active site. The fact that catalyst decomposition was not observed spectroscopically (Figure 9) is not contradictory with the water-induced decomposition of the catalyst during the reaction: as shown by DeKock et al.,[46] Wacker-type reactions (involving the participation of C_2H_4) are a likely culprit

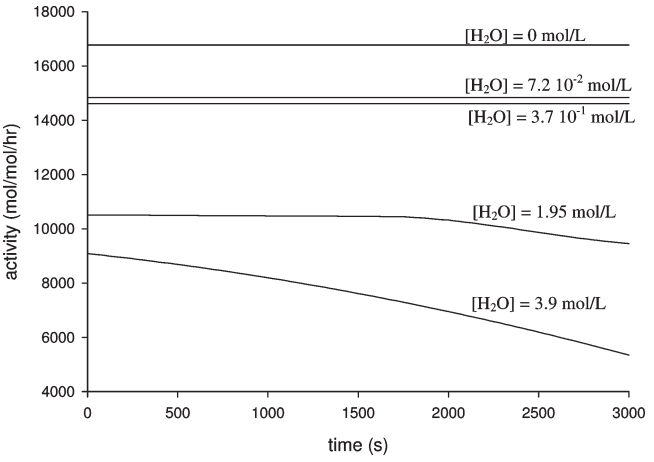

Figure 10. Catalytic activity (TOF) for the homopolymerization of ethylene by **3** in THF containing various amounts of water (T = 85 °C, [**3**] = 5.2 μmol/L, P = 300 psi).

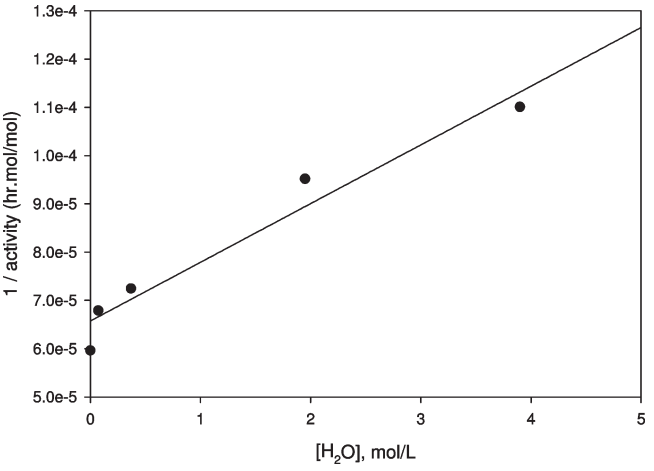

Figure 11. Inverse of the initial activity vs water concentration in THF (experiments of Figure 10, T = 85 °C, [**3**] = 5.2 μmol/L, P = 300 psi).

for the decomposition of the catalyst. For catalyst **3**, the decomposition reaction becomes noticeable only after prolonged reaction times, whereas coordination of water is reducing the activity in a constant manner throughout the reaction duration. Both of these factors are expected to be at play for polymerization in emulsion with catalysts **2a** and **2b**; however, their precise magnitude is unknown at this time.

4. Conclusion

We have reported for the first time the preparation of latexes of poly(ethylene-*co*-acrylate) made by catalytic emulsion polymerization. These latexes are colloidally stable and are expected to present interesting properties that will be explored in the future. However, their preparation is hampered by the low activity of these catalysts in an aqueous environment. This low activity originates from the combination of three factors. First pyridine is strongly bound to the catalyst: at a pressure of 300 psi in toluene less than 5% of the catalyst is bound to C_2H_4 (Table 2). This quantity is expected to further decrease in an aqueous environment because at the same pressure the solubility of ethylene is lower. Second, when an acrylate is present, it coordinates both in a π- and σ-fashion. Therefore, an acrylate is not only a monomer but also an inhibitor of the catalyst. Consequently, high acrylate incorporations are achieved only to the detriment of the catalytic activity. Last, water also acts as a poison, both by coordination to Pd and by irreversible deactivation of the Pd alkyl, as already shown for other complexes by DeKock et al.[46,47] The precise contribution of each of these factors to the deactivation of the catalyst in our systems is not known at this time, and it is probably highly dependent on the reaction conditions.

Another important feature of this work is the discovery that the ligand substitution occurs via an associative pathway. Retrospectively, an associative mechanism for ligand susbstitution has already been extensively demonstrated for simple coordination complexes.[48] Unlike cationic palladium diimines for which the associative mechanism has been found to play a pivotal role in the regulation of molecular weight, the associative nature of the ligand substitution reaction has often been overlooked for neutral Ni and Pd polymerization catalysts. As a corollary, for the determination of complexation energies, either experimentally or by DFT studies, both associative and dissociative mechanisms should be probed. In the future we intend to measure such complexation energies for complexes having sterically hindered axial faces (such as **3**), in order to assess whether the substitution still occurs by an associative mechanism or whether a dissociative route is followed.

Acknowledgment. This work was supported by the U.S. DoC (NIST, Advanced Technology Program, Cooperative Agreement 70NANB4H3014), the NSF (Goali Grant 0354825), NSERC Discovery Program, and the Canadian Foundation for Innovation. We thank Mr. Daigle for technical help.

Supporting Information Available: Derivation of the analytical expression for TOF and details on the determination of k_1, k_2, and k_{-1}. This material is available free of charge via the Internet at http://pubs.acs.org/.

References and Notes

(1) Fitch, R. M. *Polymer Colloids: A Comprehensive Introduction*; Academic Press: San Diego, 1997.
(2) Lowell, P. A.; El-Aasser, M. S. *Emulsion Polymerization and Emulsion Polymers*; John Wiley: Chichester, 1997.
(3) Soula, R.; Broyer, J. P.; Llauro, M. F.; Tomov, A.; Spitz, R.; Claverie, J.; Drujon, X.; Malinge, J.; Saudemont, T. *Macromolecules* **2001**, *34* (8), 2438–2442.
(4) Soula, R.; Novat, C.; Tomov, A.; Spitz, R.; Claverie, J.; Drujon, X.; Malinge, J.; Saudemont, T. *Macromolecules* **2001**, *34* (7), 2022–2026.
(5) Soula, R.; Saillard, B.; Spitz, R.; Claverie, J.; Llaurro, M. F.; Monnet, C. *Macromolecules* **2002**, *35* (5), 1513–1523.
(6) Claverie, J. P.; Soula, R. *Prog. Polym. Sci.* **2003**, *28* (4), 619–662.
(7) Mecking, S.; Claverie, J. P. Transition metal-catalyzed polymerization in aqueous systems. In *Late Transition Metal Polymerization Catalysis*; Rieger, B., Baugh, L. S., Kacker, S., Striegler, S., Eds.; Wiley-VCH: Weinheim, 2003; pp 231−278.
(8) Soula, R.; Claverie, J.; Spitz, R.; Guyot, A. *Surfactant Sci. Ser.* **2003**, *115*, 77–92.
(9) Bauers, F. M.; Mecking, S. *Macromolecules* **2001**, *34* (5), 1165–1171.
(10) Mecking, S.; Held, A.; Bauers, F. M. *Angew. Chem., Int. Ed.* **2002**, *41* (4), 544–561.
(11) Bauers, F. M.; Chowdhry, M. M.; Mecking, S. *Macromolecules* **2003**, *36* (18), 6711–6715.
(12) Bauers, F. M.; Thomann, R.; Mecking, S. *J. Am. Chem. Soc.* **2003**, *125* (29), 8838–8840.
(13) Kolb, L.; Monteil, V.; Thomann, R.; Mecking, S. *Angew. Chem., Int. Ed.* **2005**, *44* (3), 429–432.
(14) Mecking, S. *Colloid Polym. Sci.* **2007**, *285* (6), 605–619.
(15) Skupov, K. M.; Marella, P. R.; Hobbs, J. L.; McIntosh, L. H.; Goodall, B. L.; Claverie, J. P. *Macromolecules* **2006**, *39* (13), 4279–4281.
(16) Skupov, K. M.; Hobbs, J.; Claverie, J. P. *Prog. Org. Coat.* **2009**, *65* (3), 314–321.
(17) Skupov, K. M.; Piche, L.; Claverie, J. P. *Macromolecules* **2008**, *41* (7), 2309–2310.

(18) Johnson, L. K.; Mecking, S.; Brookhart, M. *J. Am. Chem. Soc.* **1996**, *118* (1), 267–268.
(19) Popeney, C. S.; Camacho, D. H.; Guan, Z. *J. Am. Chem. Soc.* **2007**, *129* (33), 10062–10063.
(20) Drent, E.; van Dijk, R.; van Ginkel, R.; van Oort, B.; Pugh, R. I. *Chem. Commun.* **2002**, *7*, 744–745.
(21) Hearley, A. K.; Nowack, R. J.; Rieger, B. *Organometallics* **2005**, *24* (11), 2755–2763.
(22) Allen, N. T.; Goodall, B. L.; McIntosh, L. H. Substantially Linear Polymers and Methods of Making and Using Same. US 2007/049712 A1, July 17, **2006**.
(23) Goodall, B. L.; Allen, N. T.; Conner, D. M.; Kirk, T. C.; McIntosh, L. H.; Shen, H. *Polym. Prepr.* (*Am. Chem. Soc., Div. Polym. Chem.*) **2007**, *48* (1), 202.
(24) Kochi, T.; Yoshimura, K.; Nozaki, K. *Dalton Trans.* **2005**, No. 1, 25–27.
(25) Kochi, T.; Noda, S.; Yoshimura, K.; Nozaki, K. *J. Am. Chem. Soc.* **2007**, *129* (29), 8948–8949.
(26) Liu, S.; Borkar, S.; Newsham, D.; Yennawar, H.; Sen, A. *Organometallics* **2007**, *26* (1), 210–216.
(27) Skupov, K. M.; Marella, P. R.; Simard, M.; Yap, G. P. A.; Allen, N.; Conner, D.; Goodall, B. L.; Claverie, J. P. *Macromol. Rapid Commun.* **2007**, *28* (20), 2033–2038.
(28) Luo, S.; Vela, J.; Lief, G. R.; Jordan, R. F. *J. Am. Chem. Soc.* **2007**, *129* (29), 8946–8947.
(29) Borkar, S.; Newsham, D. K.; Sen, A. *Organometallics* **2008**, *27* (14), 3331–3334.
(30) Vela, J.; Lief, G. R.; Shen, Z.; Jordan, R. F. *Organometallics* **2007**, *26* (26), 6624–6635.
(31) Guironnet, D.; Roesle, P.; Ruenzi, T.; Gottker-Schnetmann, I.; Mecking, S. *J. Am. Chem. Soc.* **2009**, *131* (2), 422–423.
(32) De Graaf, W.; Boersma, J.; Smeets, W. J. J.; Spek, A. L.; Van Koten, G. *Organometallics* **1989**, *8* (12), 2907–2917.
(33) Bain, A. D.; Duns, G. J. *Can. J. Chem.* **1996**, *74*, 819–824.
(34) Castellano, S.; Sun, C.; Kostelnik, R. *J. Chem. Phys.* **1967**, *46* (1), 327–330.
(35) Reich, H. J.; Goldenberg, W. S.; Gudmundsson, B. O.; Sanders, A. W.; Kulicke, K. J.; Simon, K.; Guzei, I. A. *J. Am. Chem. Soc.* **2001**, *123* (33), 8067–8079.
(36) Mecking, S.; Johnson, L. K.; Wang, L.; Brookhart, M. *J. Am. Chem. Soc.* **1998**, *120* (5), 888–899.
(37) Shamsipur, M.; Karkhaneeib, E.; Afkhamib, A. *Polyhedron* **1998**, *17* (21), 3809–3815.
(38) Cahen, Y. M.; Dye, J. L.; Popov, A. I. *J. Phys. Chem.* **1975**, *73* (13), 1292–1295.
(39) Pons, M.; Millet, O. *Prog. Nucl. Magn. Reson. Spectrosc.* **2001**, *38*, 267–324.
(40) Michalak, A.; Ziegler, T. *Organometallics* **2003**, *22* (10), 2069–2079.
(41) Michalak, A.; Ziegler, T. *Organometallics* **2000**, *19* (10), 1850–1858.
(42) Landfester, K.; Bechthold, N.; Tiarks, F.; Antonietti, M. *Macromolecules* **1999**, *32* (16), 5222–5228.
(43) Bradbury, E. J.; McNulty, D.; Savage, R. L.; McSweeney, E. E. *Ind. Eng. Chem.* **1952**, *44* (1), 211–212.
(44) Bechthold, N.; Tiarks, F.; Willert, M.; Landfester, K.; Antonietti, M. *Macromol. Symp.* **2000**, *151* (1), 549–555.
(45) Monteil, V.; Wehrmann, P.; Mecking, S. *J. Am. Chem. Soc.* **2005**, *127* (42), 14568–14569.
(46) DeKock, R. L.; Hristov, I. H.; Anderson, G. D. W.; Gottker-Schnetmann, I.; Mecking, S.; Ziegler, T. *Organometallics* **2005**, *24* (11), 2679–2687.
(47) Hristov, I. H.; DeKock, R. L.; Anderson, G. D. W.; Gottker-Schnetmann, I.; Mecking, S.; Ziegler, T. *Inorg. Chem.* **2005**, *44* (22), 7806–7818.
(48) Atwood, J. D. *Inorganic and Organometallic Reaction Mechanisms*, 2nd ed.; Wiley-VCH: New York, 1997.